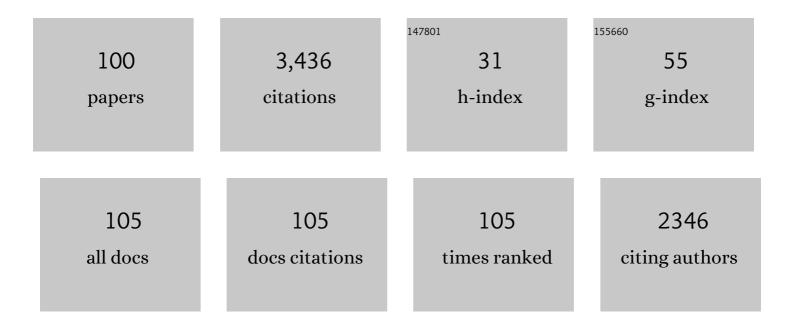
## Nathalie Bozzolo

List of Publications by Year in descending order

Source: https://exaly.com/author-pdf/6684874/publications.pdf Version: 2024-02-01



#	Article	IF	CITATIONS
1	Analysis of the tensile behavior of a TWIP steel based on the texture and microstructure evolutions. Materials Science & Engineering A: Structural Materials: Properties, Microstructure and Processing, 2009, 500, 196-206.	5.6	404
2	Annealing twin development during recrystallization and grain growth in pure nickel. Materials Science & Engineering A: Structural Materials: Properties, Microstructure and Processing, 2014, 597, 295-303.	5.6	175
3	Evolution of recrystallisation texture and microstructure in low alloyed titanium sheets. Acta Materialia, 2002, 50, 1245-1259.	7.9	160
4	About quantitative EBSD analysis of deformation and recovery substructures in pure Tantalum. IOP Conference Series: Materials Science and Engineering, 2015, 89, 012038.	0.6	110
5	Selective Growth of Low Stored Energy Grains During δSub-solvus Annealing in the Inconel 718 Nickel-Based Superalloy. Metallurgical and Materials Transactions A: Physical Metallurgy and Materials Science, 2015, 46, 4405-4421.	2.2	99
6	Texture evolution during grain growth in recrystallized commercially pure titanium. Materials Science & Engineering A: Structural Materials: Properties, Microstructure and Processing, 2005, 397, 346-355.	5.6	97
7	Evolution of microstructure and twin density during thermomechanical processing in a γ-γ' nickel-based superalloy. Acta Materialia, 2012, 60, 5056-5066.	7.9	97
8	Statistical analysis of dislocations and dislocation boundaries from EBSD data. Ultramicroscopy, 2017, 179, 63-72.	1.9	95
9	Influence of strain rate on subsolvus dynamic and post-dynamic recrystallization kinetics of Inconel 718. Acta Materialia, 2019, 174, 406-417.	7.9	94
10	The mechanisms of microstructure formation in a nanostructured oxide dispersion strengthened FeAl alloy obtained by spark plasma sintering. Intermetallics, 2007, 15, 108-118.	3.9	87
11	Misorientations induced by deformation twinning in titanium. Journal of Applied Crystallography, 2010, 43, 596-602.	4.5	84
12	Mean field modelling of dynamic and post-dynamic recrystallization during hot deformation of Inconel 718 in the absence of δ phase particles. Materials Science & Engineering A: Structural Materials: Properties, Microstructure and Processing, 2016, 655, 408-424.	5.6	79
13	Observation of annealing twin nucleation at triple lines in nickel during grain growth. Acta Materialia, 2015, 99, 63-68.	7.9	73
14	Microstructure and microtexture of highly cold-rolled commercially pure titanium. Journal of Materials Science, 2007, 42, 2405-2416.	3.7	72
15	Heteroepitaxial recrystallization: A new mechanism discovered in a polycrystalline γ-γ′ nickel based superalloy. Journal of Alloys and Compounds, 2016, 688, 685-694.	5.5	62
16	About the possibility of grain boundary engineering via hot-working in a nickel-base superalloy. Scripta Materialia, 2010, 62, 851-854.	5.2	61
17	Viewpoint on the Formation and Evolution of Annealing Twins During Thermomechanical Processing of FCC Metals and Alloys. Metallurgical and Materials Transactions A: Physical Metallurgy and Materials Science, 2020, 51, 2665-2684.	2.2	61
18	Formation of Annealing Twins during Recrystallization and Grain Growth in 304L Austenitic Stainless Steel, Materials Science Forum, 0, 753, 113-116.	0.3	54

#	Article	IF	CITATIONS
19	EBSD for analysing the twinning microstructure in fineâ€grained TWIP steels and its influence on work hardening. Journal of Microscopy, 2009, 235, 67-78.	1.8	53
20	New finite element developments for the full field modeling of microstructural evolutions using the level-set method. Computational Materials Science, 2015, 109, 388-398.	3.0	52
21	Modeling of dynamic and post-dynamic recrystallization by coupling a full field approach to phenomenological laws. Materials and Design, 2017, 133, 498-519.	7.0	50
22	Observations on the effect of a magnetic field on the annealing texture and microstructure evolution in zirconium. Acta Materialia, 2010, 58, 3568-3581.	7.9	49
23	Development of a level set methodology to simulate grain growth in the presence of real secondary phase particles and stored energy – Application to a nickel-base superalloy. Computational Materials Science, 2014, 89, 233-241.	3.0	49
24	3D level set modeling of static recrystallization considering stored energy fields. Computational Materials Science, 2016, 122, 57-71.	3.0	48
25	Low Temperature Tempering of a Medium Carbon Steel in High Magnetic Field. ISIJ International, 2005, 45, 913-917.	1.4	45
26	Overgrown grains appearing during sub-solvus heat treatment in a polycrystalline γ-γ' Nickel-based superalloy. Materials and Design, 2018, 144, 353-360.	7.0	44
27	Thermo-mechanical factors influencing annealing twin development in nickel during recrystallization. Journal of Materials Science, 2015, 50, 5191-5203.	3.7	43
28	Fast in-situ annealing stage coupled with EBSD: A suitable tool to observe quick recrystallization mechanisms. Materials Characterization, 2012, 70, 28-32.	4.4	41
29	About texture stability during primary recrystallization of cold-rolled low alloyed zirconium. Scripta Materialia, 2009, 60, 203-206.	5.2	40
30	A New Approach to Modeling the Flow Curve of Hot Deformed Austenite. ISIJ International, 2011, 51, 945-950.	1.4	38
31	Evidence of multimicrometric coherent γ′ precipitates in a hotâ€forged γ–γ′ nickelâ€based superalloy. Jo of Microscopy, 2016, 263, 106-112.	ournal 1.8	34
32	Discrimination of dynamically and postâ€dynamically recrystallized grains based on EBSD data: application to Inconel 718. Journal of Microscopy, 2019, 273, 135-147.	1.8	33
33	In Situ Characterization of Inconel 718 Post-Dynamic Recrystallization within a Scanning Electron Microscope. Metals, 2017, 7, 476.	2.3	32
34	A novel level-set finite element formulation for grain growth with heterogeneous grain boundary energies. Materials and Design, 2018, 160, 578-590.	7.0	32
35	Strain Induced Abnormal Grain Growth in Nickel Base Superalloys. Materials Science Forum, 2013, 753, 321-324.	0.3	31
36	On the Coupling between Recrystallization and Precipitation Following Hot Deformation in a γ-γ′ Nickel-Based Superalloy. Metallurgical and Materials Transactions A: Physical Metallurgy and Materials Science, 2018, 49, 4199-4213.	2.2	31

#	Article	IF	CITATIONS
37	Estimation of geometrically necessary dislocation density from filtered EBSD data by a local linear adaptation of smoothing splines. Journal of Applied Crystallography, 2019, 52, 548-563.	4.5	30
38	Carbothermal Transformation of TiO <sub>2</sub> into TiO <sub><i>x</i></sub> C <sub><i>y</i></sub> in UHV: Tracking Intrinsic Chemical Stabilities. Journal of Physical Chemistry C, 2014, 118, 22601-22610.	3.1	29
39	2D finite element modeling of misorientation dependent anisotropic grain growth in polycrystalline materials: Level set versus multi-phase-field method. Computational Materials Science, 2015, 104, 108-123.	3.0	29
40	Evolution of the Annealing Twin Density during δ-Supersolvus Grain Growth in the Nickel-Based Superalloy Inconelâ,,¢ 718. Metals, 2016, 6, 5.	2.3	29
41	Accuracy of orientation distribution function determination based on EBSD data-A case study of a recrystallized low alloyed Zr sheet. Journal of Microscopy, 2007, 227, 275-283.	1.8	27
42	Hardness, thermal stability and yttrium distribution in nanostructured deposits obtained by thermal spraying from milled—Y2O3 reinforced—or atomized FeAl powders. Intermetallics, 2006, 14, 715-721.	3.9	25
43	Nucleation mechanism of hetero-epitaxial recrystallization in wrought nickel-based superalloys. Scripta Materialia, 2021, 191, 7-11.	5.2	23
44	Magnetically affected texture and grain structure development in titanium. Materials Letters, 2005, 59, 3209-3213.	2.6	21
45	A new topological approach for the mean field modeling of dynamic recrystallization. Materials and Design, 2018, 146, 194-207.	7.0	21
46	EBSD coupled to SEM <i>in situ</i> annealing for assessing recrystallization and grain growth mechanisms in pure tantalum. Journal of Microscopy, 2013, 250, 189-199.	1.8	20
47	Consequences of a Room-Temperature Plastic Deformation During Processing on Creep Durability of a Ni-Based SX Superalloy. Metallurgical and Materials Transactions A: Physical Metallurgy and Materials Science, 2018, 49, 4246-4261.	2.2	20
48	A 2D level set finite element grain coarsening study with heterogeneous grain boundary energies. Applied Mathematical Modelling, 2020, 78, 505-518.	4.2	19
49	Influence of the strain path changes on the formability of a zinc sheet. Journal of Materials Processing Technology, 2019, 271, 101-110.	6.3	17
50	On the evaluation of dislocation densities in pure tantalum from EBSD orientation data. Materiaux Et Techniques, 2018, 106, 604.	0.9	17
51	Grain Growth Texture Evolution in Zirconium (Zr702) and Commercially Pure Titanium (T40). Materials Science Forum, 2004, 467-470, 441-446.	0.3	16
52	Experimental Investigations of Recrystallization Texture Development in Zirconium (Zr702). Materials Science Forum, 2004, 467-470, 453-458.	0.3	16
53	Full field modeling of recrystallization: Effect of intragranular strain gradients on grain boundary shape and kinetics. Computational Materials Science, 2018, 150, 149-161.	3.0	16
54	Crystalline quality of highly oriented diamond films grown on ã€^100〉 silicon studied by conventional TEM. Diamond and Related Materials, 1997, 6, 41-47.	3.9	14

#	Article	IF	CITATIONS
55	Recrystallization Textures in some Hexagonal Alloys. Materials Science Forum, 2002, 408-412, 901-906.	0.3	14
56	Improvement of 3D mean field models for capillarity-driven grain growth based on full field simulations. Journal of Materials Science, 2016, 51, 10970-10981.	3.7	14
57	Dissolution of the Primary γ′ Precipitates and Grain Growth during Solution Treatment of Three Nickel Base Superalloys. Metals, 2021, 11, 1921.	2.3	14
58	γ′ precipitates with a twin orientation relationship to their hosting grain in a γ-γ′ nickel-based superalloy. Scripta Materialia, 2018, 153, 10-13.	5.2	13
59	Statistical behaviour of interfaces subjected to curvature flow and torque effects applied to microstructural evolutions. Acta Materialia, 2022, 222, 117459.	7.9	13
60	Microstructure evolution and thermal stability of equiatomic CoCrFeNi films on (0001) α-Al2O3. Acta Materialia, 2020, 200, 908-921.	7.9	12
61	Nanocrystalline equiatomic CoCrFeNi alloy thin films: Are they single phase fcc?. Surface and Coatings Technology, 2021, 410, 126945.	4.8	12
62	Phase discrimination between δ and Ε phases in the new nickel-based superalloy VDM Alloy 780 using EBSD. Materials Characterization, 2021, 176, 111105.	4.4	12
63	A metallurgical approach to individually assess the rheology of alpha and beta phases of Ti–6Al–4V in the two-phase domain. Materials Characterization, 2014, 89, 88-92.	4.4	11
64	A Mechanism Leading to γ′ Precipitates with {111} Facets and Unusual Orientation Relationships to the Matrix in γ–γ′ Nickel-Based Superalloys. Metallurgical and Materials Transactions A: Physical Metallurgy and Materials Science, 2018, 49, 4308-4323.	2.2	11
65	Full field modeling of dynamic recrystallization in a CPFEM context – Application to 304L steel. Computational Materials Science, 2020, 184, 109892.	3.0	11
66	Chemical redistribution and change in crystal lattice parameters during stress relaxation annealing of the AD730TM superalloy. Acta Materialia, 2022, 237, 118141.	7.9	11
67	Grain Boundary Character Evolution during Grain Growth in a Zr Alloy. Materials Science Forum, 2007, 558-559, 863-868.	0.3	10
68	iCHORD-SI combination as an alternative to EDS-EBSD coupling for the characterization of γ-γ′ nickel-based superalloy microstructures. Materials Characterization, 2018, 142, 492-503.	4.4	10
69	A level set approach to simulate grain growth with an evolving population of second phase particles. Modelling and Simulation in Materials Science and Engineering, 2021, 29, 035009.	2.0	10
70	Substrate Grain-Dependent Chemistry of Carburized Planar Anodic TiO <sub>2</sub> on Polycrystalline Ti. ACS Omega, 2017, 2, 631-640.	3.5	9
71	Comparative Study and Limits of Different Level-Set Formulations for the Modeling of Anisotropic Grain Growth. Materials, 2021, 14, 3883.	2.9	9
72	Physical and chemical analyses on single source precursor growth CdSe semiconductor nanomaterials. Materials Chemistry and Physics, 2010, 124, 129-133.	4.0	7

#	Article	IF	CITATIONS
73	Advances in Level-Set Modeling of Recrystallization at the Polycrystal Scale - Development of the Digi- <i>î¼</i> Software. Key Engineering Materials, 0, 651-653, 617-623.	0.4	7
74	Electron backscatter diffraction study of orientation gradients at the grain boundaries of a polycrystalline steel sheet deformed along different loading paths. Journal of Applied Crystallography, 2017, 50, 1179-1191.	4.5	7
75	A new analytical test case for anisotropic grain growth problems. Applied Mathematical Modelling, 2021, 93, 28-52.	4.2	7
76	Dynamic and Post-dynamic Recrystallization During Supersolvus Forging of the New Nickel-Based Superalloy—VDM Alloy 780. Minerals, Metals and Materials Series, 2020, , 450-460.	0.4	7
77	Effect of Recrystallization on Tensile Behavior, Texture, and Anisotropy of Ti-3Al-2.5 V Cold Pilgered Tubes. Advanced Engineering Materials, 2011, 13, 383-387.	3.5	6
78	Fabrication of Ti substrate grain dependent C/TiO <sub>2</sub> composites through carbothermal treatment of anodic TiO <sub>2</sub> . Physical Chemistry Chemical Physics, 2016, 18, 9220-9231.	2.8	6
79	Spatial distribution of stacking faults and microtwins in isolated crystals and textured diamond films. Diamond and Related Materials, 1996, 5, 1532-1535.	3.9	5
80	Some Remarks about the Processing of Automatic EBSD Orientation Measurements in View of Texture Determination. Materials Science Forum, 2002, 408-412, 143-148.	0.3	5
81	Crystal orientation distribution in highly oriented diamond films investigated by SEM and TEM. Diamond and Related Materials, 2006, 15, 531-535.	3.9	5
82	Magnetically Affected Texture and Microstructure Evolution during Grain Growth in Zirconium. Materials Science Forum, 2012, 715-716, 946-951.	0.3	5
83	Evolution of Microstructure in Pure Nickel during Processing for Grain Boundary Engineering. Materials Science Forum, 2013, 753, 97-100.	0.3	4
84	Multipass forging of Inconel 718 in the delta-Supersolvus domain: assessing and modeling microstructure evolution. MATEC Web of Conferences, 2014, 14, 12001.	0.2	4
85	A mean field model of agglomeration as an extension to existing precipitation models. Acta Materialia, 2020, 192, 40-51.	7.9	4
86	An Optimized Geometry of Double-Cone Compression Test Samples for a Better Control of Strain Rate. Metallurgical and Materials Transactions A: Physical Metallurgy and Materials Science, 2021, 52, 4125-4136.	2.2	4
87	Influence of Deformation Substructures on the Early Mechanisms of Recrystallization in Cold-Rolled Titanium and Zirconium. Materials, Science Forum, 2005, 495-497, 711-718, Growth and Orientation relationships of Ni and Cu films annealed on slightly miscut <mml:math< td=""><td>0.3</td><td>3</td></mml:math<>	0.3	3
88	xmlns:mml="http://www.w3.org/1998/Math/MathML" altimg="si4.gif" overflow="scroll"> <mml:mrow><mml:mo stretchy="false"&gt;(<mml:mn>1</mml:mn><mml:mspace )="" 0="" etqq0="" overlock<="" rgbt="" td="" tj="" width="5.0pt"><td>≀ 101<b>⊺\$</b> 50 1</td><td>1373Td (/&gt;<m< td=""></m<></td></mml:mspace></mml:mo </mml:mrow>	≀ 101 <b>⊺\$</b> 50 1	1373Td (/> <m< td=""></m<>
89	Introduction to the level-set full field modeling of laths spheroidization phenomenon in α/β titanium alloys. International Journal of Material Forming, 2019, 12, 173-183.	2.0	3

 $90 \qquad \mbox{Heteroepitaxial Recrystallization, a New Recrystallization Mechanism in Sub-Solvus Forged $\hat{1}^3.\hat{1}^3 \hat{a} \in \mathbb{M}$ Nickel-Based Superalloys with Low Lattice Mismatch., 2016, , 259-264.}$ 

n

#	Article	IF	CITATIONS
91	Introduction to the level-set full field modeling of laths spheroidization phenomenon in $\hat{l}\pm/\hat{l}^2$ titanium alloys. MATEC Web of Conferences, 2016, 80, 02003.	0.2	2
92	Prediction of the grain size evolution during thermal treatments at the mesoscopic scale: a numerical framework and industrial examples. Materiaux Et Techniques, 2018, 106, 105.	0.9	2
93	Level-Set Modeling of Grain Growth in 316L Stainless Steel under Different Assumptions Regarding Grain Boundary Properties. Materials, 2022, 15, 2434.	2.9	2
94	Formation of Coarse Recrystallized Grains in 6016 Aluminum Alloy During Holding After Hot Deformation. Metallurgical and Materials Transactions A: Physical Metallurgy and Materials Science, 2022, 53, 2402-2425.	2.2	2
95	Modeling the Evolution of Orientation Distribution Functions during Grain Growth of some Ti and Zr Alloys. Materials Science Forum, 2007, 558-559, 1163-1168.	0.3	1
96	Recrystallisation Behavior of Cold Rolled Zr702: Influence of Rolling Direction and Thickness Reduction. Materials Science Forum, 2007, 550, 459-464.	0.3	1
97	Effect of Thermomechanical Processes on Σ3 Grain Boundary Distribution in a Nickel Base Superalloy. Materials Science Forum, 2010, 638-642, 2333-2338.	0.3	1
98	Textures in HCP Titanium and Zirconium: Influence of Twinning. Ceramic Transactions, 0, , 461-472.	0.1	1
99	EBSD Coupled to SEM <i>In Situ</i> Annealing as a Tool to Identify Recrystallization Mechanisms - Application to Zr and Ta Alloys. Materials Science Forum, 0, 715-716, 486-491.	0.3	Ο
100	On the Stability of Recrystallization Textures in Low Alloyed Zirconium Sheets. Ceramic Transactions, 0, , 429-436.	0.1	0